8-29-2008

Inverse Velocity Dependence of Vibrationally Promoted Electron Emission from a Metal Surface

N. H. Nahler
University of California, Santa Barbara

J. D. White
University of California, Santa Barbara

Jerry L. LaRue
Chapman University, larue@chapman.edu

Daniel J. Auerbach
University of California, Santa Barbara

Alec M. Wodtke
University of California, Santa Barbara

Recommended Citation
N. H. Nahler, J. D. White, J. LaRue, D. J. Auerbach, A. M. Wodtke, Inverse Velocity Dependence of Vibrationally Promoted Electron Emission from a Metal Surface, *Science* 2008, 321, 1191-1194, DOI: 10.1126/science.1160040

Inverse Velocity Dependence of Vibrationally Promoted Electron Emission from a Metal Surface

Inverse velocity dependence of vibrationally promoted electron emission from a metal surface

N. H. Nahler[a], J. D. White[a], J. LaRue[a], D. J. Auerbach[b], and A. M. Wodtke[a*]

[a] Department of Chemistry and Biochemistry, University of California Santa Barbara, Santa Barbara, California 93106-9510; [b] GRT Inc., 861 Ward Drive, Santa Barbara, CA 93111-2920

All previous experimental and theoretical studies of molecular interactions at metal surfaces show that electronically nonadiabatic influences increase with molecular velocity. Here, we report the observation of a nonadiabatic electronic effect that follows the opposite trend: the probability for electron emission from a low work function surface – Au(111) capped by half a monolayer of Cs – increases as the velocity of the incident NO molecule decreases in the course of collisions with highly vibrationally excited NO($X^2\Pi_{½}$, **V**=18), reaching 0.1 at the lowest velocity studied. We show these results are consistent with a vibrational auto-detachment mechanism, where electron emission is only possible beyond a certain critical distance from the surface. This outcome implies that important energy dissipation pathways involving nonadiabatic electronic excitations and furthermore not captured by present theoretical methods, may influence reaction rates at surfaces.

PACS numbers: 34.50.Dy, 82.20.Gk, 79.20.Rf, 34.50.Ez, 68.35.Ja

*Corresponding author. Electronic address: wodtke@chem.ucsb.edu, www.chem.ucsb.edu/~wodtke/groupwebpage/

Chemical processes are generally described in terms of the Born-Oppenheimer (BO) approximation where electrons move sufficiently rapidly to adjust adiabatically as the system evolves and nuclear motion is governed by an effective electronic ground-state potential energy surface (*1*). This approach, particularly in combination with density functional theory (*2*), has contributed significantly to our understanding of surface chemistry and heterogeneous catalysis (*3*, *4*). Use of the BO approximation, however, neglects electronic excitation induced by nuclear motion, which might be expected for interactions on metal surfaces where there is a continuum of low lying electronic states. If for example chemical reactions at metal surfaces were accompanied by ubiquitous electronic excitations, important energy dissipation pathways would be neglected by present theoretical approaches. This could have important consequences for predicting reaction rates – for example overemphasizing re-crossing of transition states or underestimating the importance of rapid irreversible relaxation into product wells.

There are now many well documented examples of the breakdown of the BO approximation in molecular processes at metal surfaces (*5*-*17*). These include electron emission during strongly exothermic chemisorption, a process referred to as "exoelectron emission" (*5*, *6*); vibrational energy transfer at metal surfaces (*7*-*11*); the observation of currents (termed "chemicurrents") associated with adsorption and reactions in Schottky diode and metal-insulator-metal (MIM) structures (*12*-*14*); and the emission of electrons when highly vibrationally excited NO molecules impinge on a low work function Cs(sub-ML)/Au(111) surface (*16*, *17*)(*18*). This last phenomenon, dubbed "vibrationally promoted electron emission", is a particularly direct observation of BO approximation breakdown.

Despite evidence of BO approximation breakdown, its impact on chemical reactions at surfaces remains unclear. On the one hand, it is clear that the rate of energy loss to the solid is crucial to accurately characterizing reaction conditions; however, some of the clearest examples of

BO approximation breakdown occur so improbably – for example, exoelectron emission exhibits a per-collision-probability or 10^{-7} to 10^{-4} (*19*) – that it is hard to know if the electronically nonadiabatic events they reveal are minor side channels or if they have an important influence on reactivity.

Even for processes with significant probabilities, there are reasons to question their influence on surface chemical reactions. All observations and theories of the nonadiabatic processes cited above show a decrease in excitation probability as the velocity of the molecules relative to the surface decreases. This trend toward decreasing nonadiabatic transition probability with decreasing velocity is also seen in the gas phase, for example, in the well known Landau, Zener, Stuckelberg theory and numerous experimental results on nonadiabatic transitions at curve crossings (*20*). Furthermore, the trend is expected because breakdown of the BO approximation depends on the nuclear motion being too rapid for the electrons to independently adjust. For adsorbed molecules, where the velocity relative to the surface is zero, it is thus reasonable to question the relevance of nonadiabatic processes altogether.

We report here a surprising and seemingly paradoxical observation: the probability of electron emission observed when highly vibrationally excited NO($X^2\Pi_{½}$, **V**=18) molecules strike a low work function surface increases strongly as the velocity of the incident molecules decreases. Such electron emission self evidently involves nonadiabatic electronic excitation. Yet, as we have just discussed, the probability of nonadiabatic excitation should decrease with decreasing velocity. We also present a simple model to resolve this apparent paradox. The model is based on an extension of the vibrational auto-detachment mechanism previously proposed (*17*). The model suggests that it is not the motion of the NO molecule relative to the surface but rather the relative motion of the N and O that drives the nonadiabatic electronic excitation observed.

The experimental setup has been described in detail elsewhere (*17*). Briefly, seeded supersonic pulsed molecular beams of NO in a variety of carrier gases are used to control the velocity (v) of the NO molecules. The NO molecules are prepared in vibrationally excited states of the ground $X(^2\Pi_{1/2})$ electronic state by stimulated emission pumping (SEP) (*8, 16*) and then scattered, in ultrahigh vacuum, from a low work function surface prepared by adsorbing a fraction of a ML of Cs on Au(111). The surface prepared in this way has a work function of 1.61 ± 0.08 eV (*21*). Individual measurements of emitted electrons are carried out over only a few seconds, always within 20 minutes after surface preparation using a micro-channel plate assembly (MCP) (*22*), conditions that ensure the cleanliness and stability of the low work function surface. The electron currents are measured with a digital oscilloscope, which avoids saturation problems we had with the counting electronics used in our earlier measurements.

The basic methodology for obtaining absolute quantum yields for vibrationally promoted electron emission has been previously reported (*16, 17*). Here, we used a new method to determine the flux of vibrationally excited molecules. Briefly, we used a laser induced fluorescence (LIF) signal measured just after the molecular beam skimmer to derive the number density of NO(**V**=0) and NO(**V**=18) molecules and converted the density to beam flux using the beam velocity determined by time-of-flight methods. Finally, we used knowledge of the excitation geometry and the velocity dependent divergence of seeded beams (*23*) to determine the subsequent transmission of the NO molecules through the apparatus to the surface. We also determine the absolute flux of NO(**V**=0) from measurements of the NO partial pressure increase in the scattering chamber and the pumping speed of the vacuum system. These NO(**V**=0) measurements were also used to validate the LIF-transmission-function method used here. The transmission-function was also verified by comparison with the measurement of transmission by White et al. (*16, 17*)

In the experiment, a ns-pulsed laser excites NO to a single ro-vibrational level of the $A(^2\Sigma^+)$ state, inducing fluorescence on a ~200 ns time-scale as the molecule radiatively relaxes back to the ground electronic state (Fig. 1a). This LIF signal can be used to derive the flux of NO in **V**=0. In Fig. 1b, a second ns-pulsed laser, spatially overlapped with the first and slightly delayed, transfers population back to the ground electronic state in NO(**V**=18), depleting the LIF signal (dark shaded region). The depletion signal can be used to derive the flux of NO(**V**=18) molecules. Figures 1c and 1d show the electron signal – detected on the 100-μs time-scale – corresponding to conditions of Fig. 1a and 1b, respectively. The time dependence of the electron signal is a result of flight time from excitation to impact on the surface and thus provides precise information on the velocity distribution of the molecular beam. The electron signal of Fig. 1c is due to the impact on the surface of vibrationally excited NO resulting from Franck-Condon Pumping (FCP), i.e. spontaneous emission from $A(^2\Sigma^+)$ into a Franck-Condon distribution of vibrationally excited levels. The larger electron signal of Fig. 1d results primarily from NO(**V**=18) molecules populated by stimulated emission. The signal of Fig. 1d also contains a small contribution from FCP. Using a comparison of Fig 1a and 1b, the residual FCP signal can be accounted for in the analysis.

Fig. 2 shows the per-collision probability for electron emission (quantum yield) for NO(**V**=0) – lower panel – and NO(**V**=18) – upper panel – plotted against the inverse velocity of the molecular beam. The dashed line is a fit to the Brako-Newns model, where the positive velocity dependence of the yield is given by $e^{-v_0/v}$ (*24*). The Brako-Newns model's positive velocity dependence issues from the following physical picture. As the NO molecule approaches the surface, its lowest unoccupied molecular orbital (LUMO) is stabilized by an image charge interaction. The velocity at which the LUMO of the NO molecule passes through the Fermi level governs the energy of the LUMO at the instant it is filled by electron transfer from the surface. At high velocity the LUMO

moves far below the Fermi level before being filled creating an electronically excited state, i.e. an unoccupied hole below the Fermi level. At low velocity, the LUMO is filled by an electron close to the Fermi level and the system remains in the ground electronic state. The dashed line fit to the data of Fig. 2 for NO(**V**=0) shows that our results for the ground vibrational state conform to the velocity dependence previously reported on other systems and as such provides a validation of our experimental method (*24-26*).

The results for NO(**V**=18) – upper panel – clearly follow a different mechanism. The quantum yield of electron emission for NO(**V**=18) is many orders of magnitude larger (*27*) and has the opposite trend with velocity than that for NO(**V**=0). Over the same velocity range where the **V**=0 results increase by a factor of ~10, the **V**=18 results decrease by a similar amount. The solid line results from fitting the data to a function of the form $\mathbf{c}+\frac{\mathbf{b}}{\mathbf{v}+\mathbf{a}}$, where the best fit was found when the fitting parameters c and a are set to zero. Thus, the quantum yield for vibrationally promoted electron emission for NO(**V**=18) appears to follow a 1/v or inverse velocity dependence. How does this behavior arise?

Katz et al. have treated the problem of vibrationally promoted electron emission (*26*) by NO on Cs/Ru. Though some aspects of the experimental observations are captured in that work – for example, the positive dependence on initial vibrational excitation – like other theories of nonadiabatic interactions at surfaces, their theory predicts an increase of electron emission with increasing velocity. Their model thus does not explain the results reported here.

We have previously suggested a vibrational auto-detachment mechanism for vibrationally promoted electron emission (*17*) involving formation of a transient negative ion and auto-detachment of an electron from this transient species resulting in the transfer of vibrational energy to electronic excitation. The mechanism, illustrated in Fig. 3a, is based on the fact that the

vertical electron binding energy (VEBE) for NO varies strongly with internuclear distance; at the outer turning point (r_1) of vibrational motion for NO(**V**=18) the VEBE is about +2.2 eV – i.e. the extra electron is strongly bound – whereas at the inner turning point (r_2) it is about –2.6 eV – the extra electron is strongly repelled.

Figure 3a shows two electronic potential curves: one for NO with an electron at the Fermi level of the Cs/Au surface and one for the case where a Fermi-level electron has been transferred forming NO^-. The two curves are shifted in energy relative to their gas phase spacing by the work function, Φ, to reflect the energetics of electron transfer from the metal to the molecule when the molecule is far from the surface (*28*). For NO bond lengths, $R_{N\text{-}O} > 1.38$ Å, VEBE exceeds Φ. Thus, as the NO molecule approaches the surface, at a distance of about z~10 Å (*29*), there is sufficient overlap of the surface electron density and the LUMO of NO that it becomes possible for an electron to be transferred to the 'stretched' NO(**V**=18) molecule. For simplicity we consider only the case where this initial electron transfer occurs precisely when $R_{N\text{-}O} = 1.38$ Å, indicated by the arrow of Fig. 3a (*30*). As NO bond compression in the anion progresses, electron release from the NO may occur near the inner turning point of vibration, r_2, where the molecule's interaction with the electron is strongly repulsive – i.e. VEBE < 0. In principle, the electron may be transferred back to the surface, or it may possess sufficient kinetic energy, ΔE_2, and be ejected in the proper direction that it entirely escapes the surface and can be detected in our experiment.

Nothing in the description of the vibrational auto-detachment mechanism given so far would give rise to the 1/v velocity dependence we observe. However, a 1/v dependence could arise if three additional conditions are met: First, there must be a defined region above the surface where the electron capture step can take place, the extent of which is not dependent on the velocity of the incident NO(**V**=18); Second, the NO molecule must move with approximately constant velocity in

this region; and third, the probability of the nonadiabatic event resulting in emission of an electron must not depend on the velocity of the incident NO(**V**=18). We next discuss how these conditions can be satisfied in the auto-detachment mechanism in connection with Fig 3.

As the NO molecule approaches the surface, the NO^- curve (dashed in Fig. 3a) moves down in energy due to an image potential interaction and as a result, ΔE_2 decreases. Figure 3b shows this reduction in ΔE_2 as a function of z. Below a critical value, $z_c \sim 4.8$Å, electron emission is no longer possible because ΔE_2 becomes smaller than the work function, Φ. This establishes the first condition. Because z_c is large, the neutral NO molecule will have only weak interaction with the surface, justifying the constant velocity approximation. We take the third condition as an assumption and use it to calculate the vibrationally promoted electron emission probability, P_{vee}.

To do so, we first model the probability of the initial electron transfer to NO. The electronic coupling will depend on the overlap of the orbital of the incident NO molecule, |a> with the metal electronic states, |k> and has the form $V \sim e^{-z/\lambda}$ (*31*). Using Fermi's golden rule, the rate of electron transfer will depend on the square of *V*. To calculate P_{vee} we integrate the electron transfer rate over the trajectory of the NO molecule and multiply by the probability for a nonadiabatic transition P_{non} back to neutral NO. The trajectory includes three pieces, (i) the incoming trajectory up to the critical distance z_c, (ii) the trajectory proceeding inward and reflecting from the surface, and (iii) the outgoing trajectory from z_c outward. In principle electron emission can have contributions from regions (i) and (iii), but because the probability of NO(**V**=18) surviving reflections is small (*8*), we ignore the contribution from (iii). Using the constant velocity condition, $z = -\mathrm{v}\,t$ on the incoming trajectory

$$P_{vee} \sim P_{non} \int_{-\infty}^{-z_c/\mathrm{v}} dt[e^{\mathrm{v}t/\lambda}]^2 = \frac{\lambda}{2\mathrm{v}} P_{non} e^{-2z_c/\lambda} \qquad (1)$$

Equation (1) shows that the simple model just described does indeed reproduce the 1/v dependence observed experimentally (*32*). The 1/v dependence arises essentially from the fact that the time available for electron transfer scales as 1/v and the probability for a nonadiabatic transition P_{non} back to the neutral NO curve is independent of v. A more complete calculation would have to take into account many details that are omitted from this description. For example the electron capture might involve an electron originating at an energy, ε, below the Fermi level. For all values of ε that are energetically allowed, z_c exists and changes very little from its value for ε=0. Thus summing over the contributions from different values of ε will retain the 1/v dependence. Similar arguments can be made for generalizing the model to include loss of some vibrational energy in the inner region or transfer of the available energy to more than one electron.

The conclusions of this work strongly suggest that electronically nonadiabatic effects can play a role in bond dissociation of surface adsorbates. First, the vibrational auto-detachment mechanism described can be important whenever the LUMO is either bonding or anti-bonding. In such cases, a significant structural change between the neutral molecule and its anion implies a similar electronic-vibrational energy exchange as that represented in Fig. 3a. Only in the case where the LUMO is a nonbonding orbital is this mechanism expected to be unimportant. Furthermore, the 1/v dependence of P_{vee} in equation (1) requires that the nonadiabatic transition probability, P_{non}, be independent of v. This suggests rather directly that the motion of the center of mass of the NO molecule relative to the surface cannot be the driver of the observed nonadiabatic electronic excitation. Rather, it is the rapid stretching and compression of the N – O bond that drives the nonadiabatic dynamics. Thus the nonadiabatic couplings observed via electron emission in this work and attributed to dynamics at z □ 5Å and at finite velocities are expected to persist to small values of *z* and in the limit of zero velocity, conditions describing surface adsorb-

ates. In fact, nonadiabatic electronic coupling will only increase with decreasing values of z. More concretely, the underlying nonadiabatic excitation of electron-hole pairs represents a significant energy dissipation mechanism not accounted for by theories that employ the BO approximation. As atoms or molecular fragments react on a surface and excited electron-hole pairs are produced, the energy loss would help to rapidly stabilize the products. For example, as two recombining surface ad-atoms form an adsorbed diatomic molecule, the neglect of electron-hole pair excitation may result in an underestimate of energy dissipation to the surface, and lead to artificial re-dissociation of the diatomic in a calculation within the BO approximation. Likewise, branching between two react ions with similar activation barriers might be influenced by more efficient energy dissipation in one channel preferentially trapping a particular transition state into one product channel versus another. Hence, both reaction rate and competitive reactive branching might depend strongly on BO approximation breakdown.

The results presented here call for further work, both experimental and theoretical. The critical distance model has important experimentally testable consequences: it constrains the energy distribution of emitted electrons and predicts that vibrational relaxation would not decrease as electron emission does. A more rigorous theory of the kinetic energy dependence of vibrationally promoted electron emission is also called for. We note for example that, in the interest of simplicity, the present model neglects the possibly important role of molecular orientation. While beyond the scope of the qualitative analysis presented here, changing the charge state of a molecule can dramatically alter the orientational forces it experiences in its interaction with the metal surface. Thus, bond re-orientation of the NO molecule may play a crucial role in the vibrational auto-detachment mechanism. We hope such work will shed light more generally, on the nonadiabatic dynamics involved in dissociation, recombination, and reactions of molecules on metal surfaces (*33*).

References

1. M. Born, J. R. Oppenheimer, *Ann. Physik* **84**, 457 (1927).
2. W. Kohn, L. J. Sham, *Phys. Rev.* **140**, 1133 (1965).
3. J. Greeley, J. K. Norskov, M. Mavrikakis, *Annu. Rev. Phys. Chem.* **53**, 319 (2002).
4. K. M. Neyman, F. Illas, *Catal. Today* **105**, 2 (Jul, 2005).
5. T. Greber, *Surf. Sci. Rep.* **28**, 3 (1997).
6. H. Nienhaus, *Surf. Sci. Rep.* **45**, 3 (2002).
7. C. T. Rettner, F. Fabre, J. Kimman, D. J. Auerbach, *Phys. Rev. Lett.* **55**, 1904 (1985).
8. Y. H. Huang, C. T. Rettner, D. J. Auerbach, A. M. Wodtke, *Science* **290**, 111 (October, 2000).
9. Y. Huang, A. M. Wodtke, H. Hou, C. T. Rettner, D. J. Auerbach, *Phys. Rev. Lett.* **84**, 2985 (Mar, 2000).
10. A. M. Wodtke, J. C. Tully, D. J. Auerbach, *Int. Rev. Phys. Chem.* **23**, 513 (2004).
11. Q. Ran, D. Matsiev, D. J. Auerbach, A. M. Wodtke, *Phys. Rev. Lett.* **98**, (Jun, 2007).
12. B. Gergen, H. Nienhaus, W. H. Weinberg, E. W. McFarland, *Science* **294**, 2521 (Dec, 2001).
13. X. Z. Ji, A. Zuppero, J. M. Gidwani, G. A. Somorjai, *J. Am. Chem. Soc.* **127**, 5792 (Apr, 2005).
14. E. Hasselbrink, *Curr. Opin. Solid State Mater. Sci.* **10**, 192 (Jun-Aug, 2006).
15. D. J. Auerbach, *Science* **294**, 2488 (Dec, 2001).
16. J. D. White, J. Chen, D. Matsiev, D. J. Auerbach, A. M. Wodtke, *Nature* **433**, 503 (February, 2005).
17. J. D. White, J. Chen, D. Matsiev, D. J. Auerbach, A. M. Wodtke, *J. Chem. Phys.* **124**, 064702 (2006).
18. Here, one ML is defined as one-to-one stoichiometric equivalence of Cs to surface Au atoms.
19. T. Greber *et al.*, *Phys. Rev. B* **50**, 8755 (Sep, 1994).
20. E. E. Nikitin, *Annu. Rev. Phys. Chem.* **50**, 1 (1999).
21. J. LaRue *et al.*, *J. Chem. Phys.* **in press**, (2008).
22. Under our conditions, the work function does not change over this time scale.
23. R. T. Jongma, T. Rasing, G. Meijer, *J. Chem. Phys.* **103**, 1925 (1995).
24. R. Brako, D. M. Newns, *Rep. Prog. Phys.* **52**, 655 (1989).
25. L. Hellberg, J. Strömquist, B. Kasemo, B. I. Lundqvist, *Phys. Rev. Lett.* **74**, 4742 (Jun, 1995).
26. G. Katz, Y. Zeiri, R. Kosloff, *J. Phys. Chem. B* **109**, 18876 (October, 2005).
27. The quantum yield reported here is larger than previously reported in (16) and (17) due to detector saturation problems in the previous experiment.
28. The energetics for electron transfer to the surface become only more favorable as the molecule approaches the surface
29. One may estimate tunneling distances based on principles set forth in Ref. S3 of the supporting online material.
30. Energetically, the electron can originate from as much as 0.6 eV below the Fermi-level, but this does not meaningfully alter the analysis presented here.
31. N. Shenvi, S. Roy, P. Parandekar, J. Tully, *J. Chem. Phys.* **125**, 154703 (2006).
32. Eqn(1) is valid only in the limit of negligible depletion of the initial NO(V=18) population and thus small quantum yield. In the more general case, we must solve the differen-

tial equation for the population of NO(V=18). Eqn(1) is then the first term of a Taylor series expansion of the solution.

33. We gratefully acknowledge the financial support from National Science Foundation grant number CHE-0454806 and the Partnership for International Research and Education – for Electronic Chemistry and Catalysis at Interfaces – NSF grant number OISE-0530268. NHN acknowledges financial support through a Feodor-Lynen fellowship provided by the Alexander von Humboldt Foundation. We thank Daniel Matsiev for many useful discussions and suggestions and a critical reading of this manuscript.

Figure captions

FIGURE 1 Observed laser induced fluorescence (LIF) and electron emission signals. (a) The LIF signal induced by the $\tilde{A}$(**V**=3) ← $\tilde{X}$ (**V**=0) excitation laser is shown as a dashed line. (b) A second $\tilde{A}$(**V**=3) → $\tilde{X}$ (**V**=18) de-excitation laser induces population transfer out of the fluorescing $\tilde{A}$(**V**=3) state (shown as solid line). Note that the difference in the signals (dark shaded area) is proportional to the number of laser-prepared vibrationally excited molecules. c) The electron signal observed with only the $\tilde{A}$(**V**=3) ← $\tilde{X}$ (**V**=0) excitation laser on (shown as dashed curve). This signal arises from Franck-Condon pumping of the NO beam to a variety of excited vibrational states predominantly below **V**=13 (*17*). d) The electron signal induced by the use of both lasers (shown as a solid line). The increase in signal results from the preparation of NO ($X^2\Pi_{½}$, **V**=18).

FIGURE 2 The velocity dependence of electron emission from NO(**V**) collisions with Cs/Au surfaces: upper panel represent results for **V**=18, lower panel represent results for **V**=0. The quantum yield is plotted versus inverse velocity, Q vs. 1/v. The dashed line is a fit to the **V**=0 results using a function of the form $e^{-v_0/v}$, based on the Brako-Newns model (*24*) for chemical hole diving, v_0 = 1375 m/s. The solid lines is a fit to the **V**=18 data with a function of the form v_0/v with v_0 = 44.9 m/s. The goodness of fit is reflected in a reduced χ^2 value of 10^{-7}. The error bars reflect random errors and are 95% confidence limits based on the 'student's t-test' using 4 independent measurements at 1.65 ps/nm and 5 independent measurements at 0.403 ps/nm. While the shape of the **V**=18 quantum yield is well determined (indicated by the error bars), its absolute scaling is

subject to larger systematic errors. We estimate these systematic errors to be less than about a factor of three: e.g. $0.02<Q(2.32\ ps/nm)<0.3$.

FIGURE 3 The vibrational auto-detachment mechanism and the existence of a critical distance. (a) The potential energy curves for the NO and an electron at the Fermi level (solid curve) and NO^- (dashed curve) at infinite separation from the Cs/Au surface. The relative energies are adjusted by the work function to reflect charge transfer from the surface to the molecule and back. A highly vibrationally excited molecule may capture an electron from the surface near the outer turning point, r_1, of vibration. Note the horizontal line indicates the energy of NO(**V**=18). After NO bond compression to a bond length near 1.38 Å, an energetically adiabatic transition to the anion potential may take place, indicated by the curved arrow. The electron may then be lost from the NO molecule near the inner turning point, r_2, releasing ΔE_2. If ΔE_2 exceeds the work function, the electron may be ejected from the molecule surface system and be detected by the experimentalist at a macroscopic distance from the surface. (b) The dependence of ΔE_2 on the molecule's distance from the surface, z. The downward-pointing arrow shows the critical distance, z_c, below which ΔE_2 is less than the work function, Φ. A detailed derivation of the potentials in Figure 3 is presented in the supporting online material. A more detailed description of this mechanism has been presented in Ref. 17, especially see Fig. 10A and the discussion surrounding it.

FIGURE 1

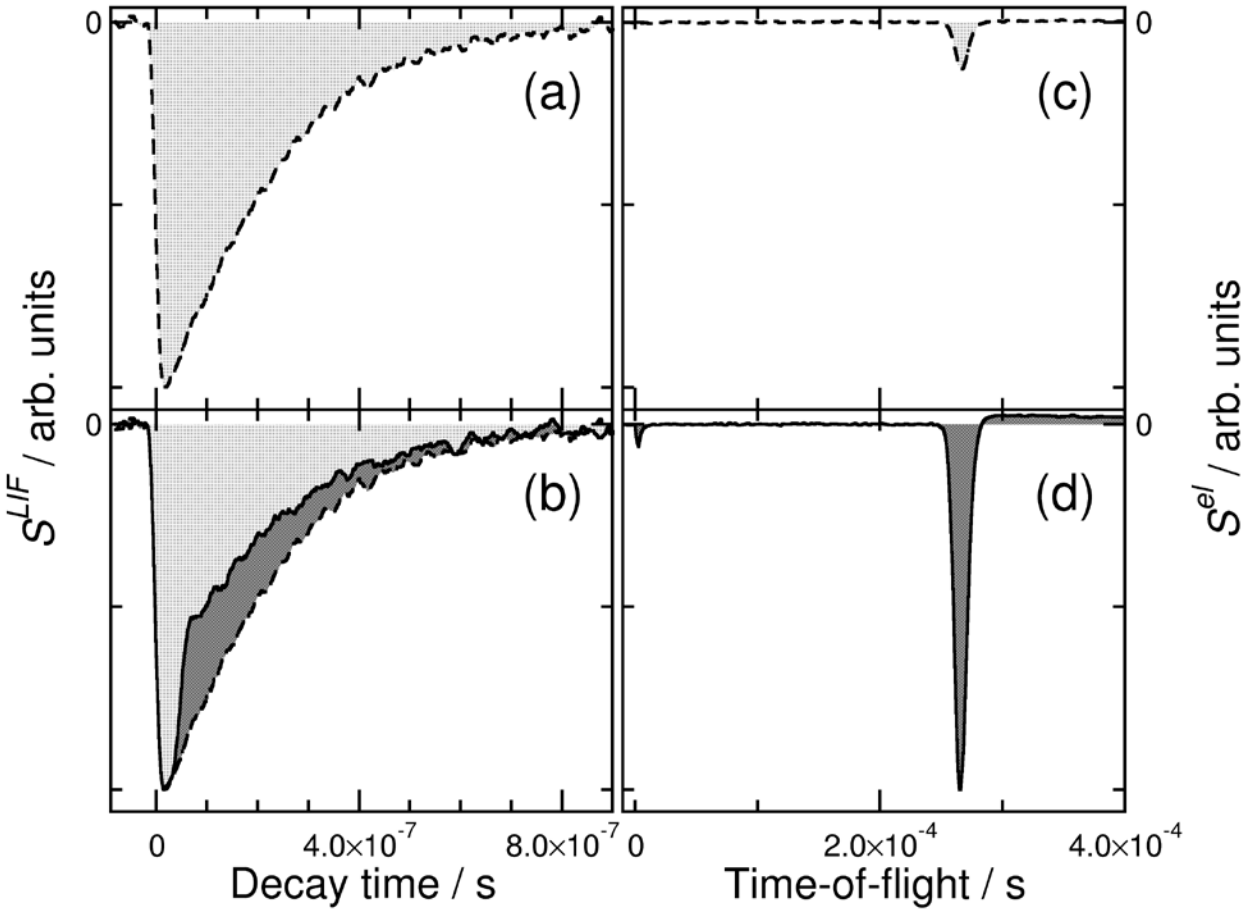
(a)
(b)
(c)
(d)
0
0
0
0
S^{LIF} / arb. units
S^{el} / arb. units
0
4.0×10^{-7}
8.0×10^{-7}
Decay time / s
0
2.0×10^{-4}
4.0×10^{-4}
Time-of-flight / s

FIGURE 2

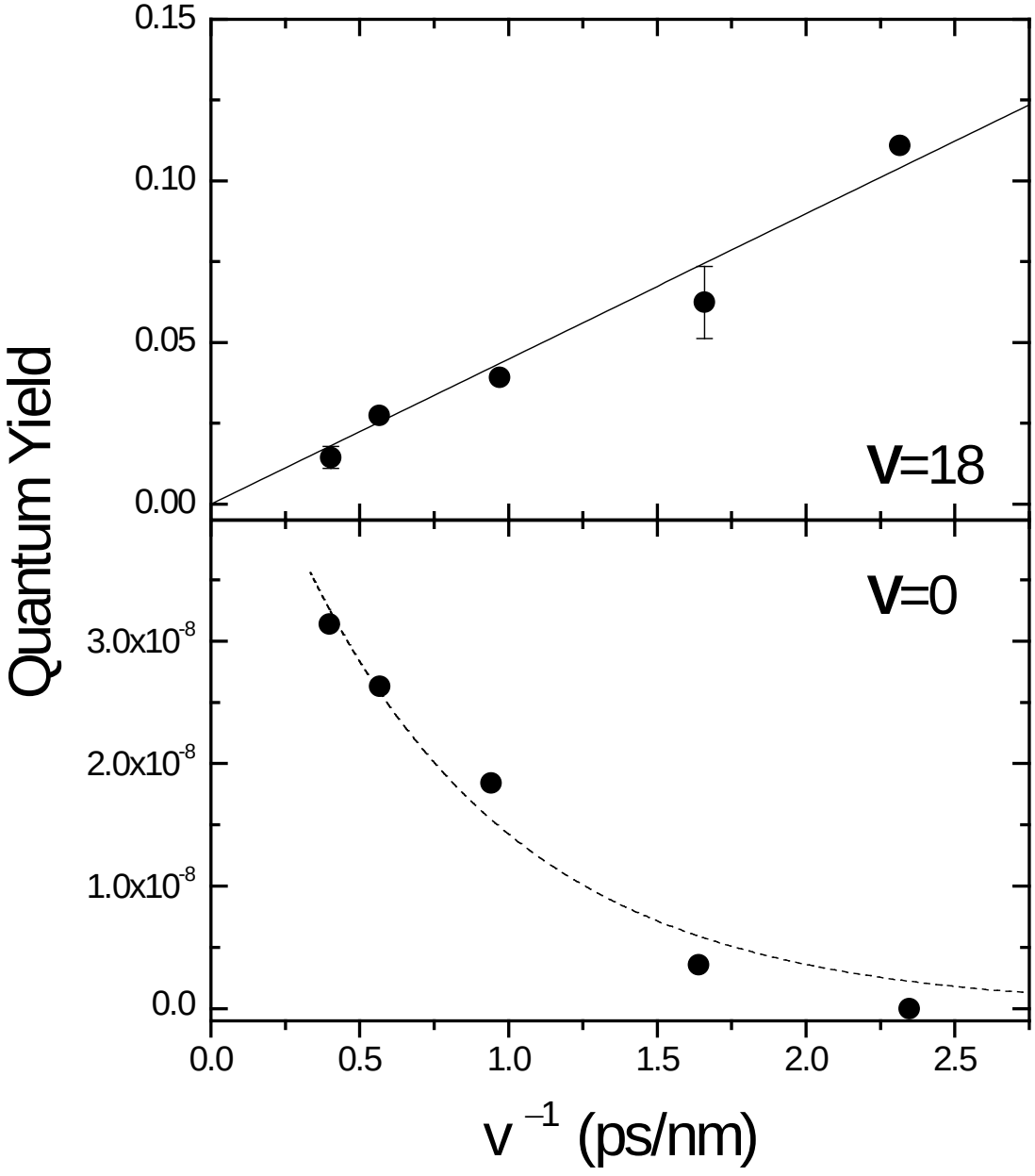
Quantum Yield
0.15
0.10
0.05
0.00
V=18
V=0
3.0x10-8
2.0x10-8
1.0x10-8
0.0
0.0
0.5
1.0
1.5
2.0
2.5
v –1 (ps/nm)

FIGURE 3

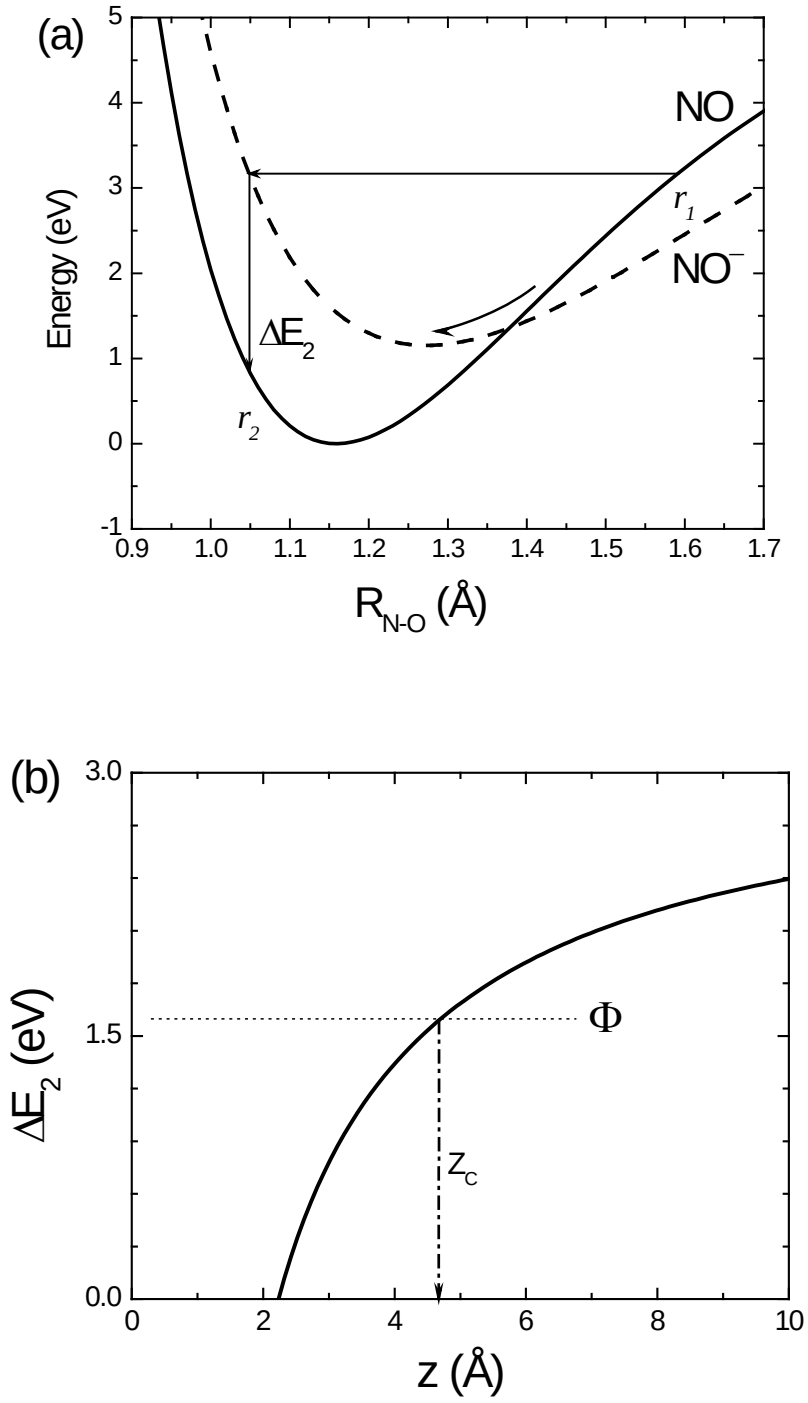

Supporting online material – Explanation of Fig. 3.

The long range interactions of NO with Cs/Au are modeled in the following way. First of all, a 2-D (r, z) coordinates system is defined, where.

r is the N-O inter-atomic distance measured in Å and

z is the distance of the surface to the CM of NO also measured in Å.

For the anion, a 2D potential (with energy units in eV) is constructed such that the r-dependence matches the NO^- inter-atomic potential obtained from *ab initio* electronic structure calculations. The plot below shows the quality of the fit to the *ab initio* points of Ref. S1.

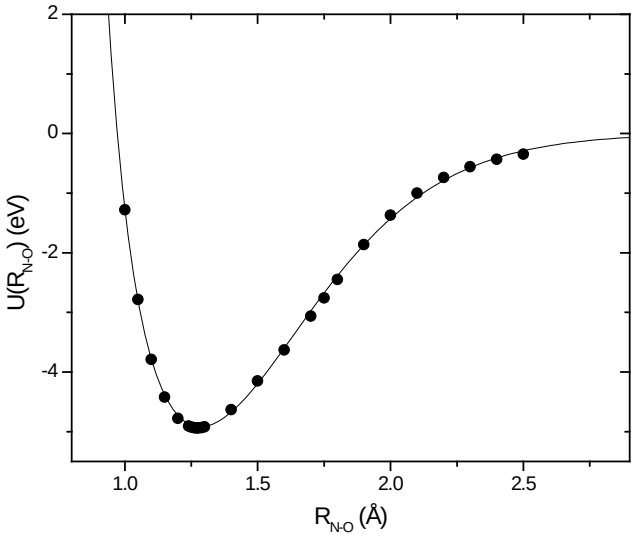

The solid line in the plot is the optimized fitting function. After shifting the origin of energy to the potential minimum, this becomes:

$$V_{anion}(r) = 4.917 - 41631.1\, e^{-5.243r}(r - 0.971816)(1.03617 + r(r - 1.81663))$$

For the z-dependence of the anion potential an image potential with a repulsive wall is used. $V_{anion}(z) = \frac{0.5}{z^{12}} - \frac{7.15109}{z}$. A plot of the z-dependence of the potential is shown below as a solid line.

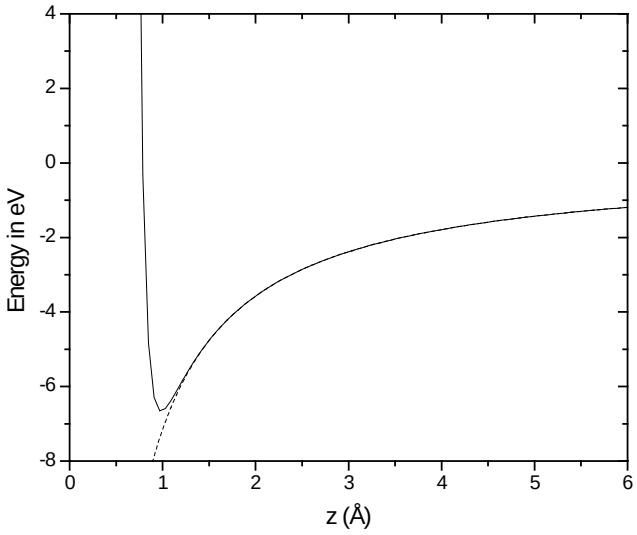

Also shown is the 1/z part of the potential as a dashed line. One should note that the influence of the repulsive contribution to the potential is not important at z>2 Å. The z and r dependent functions just described are combined as follows

$$V_{anion}(r,z) = V_{anion}(r) + V_{anion}(z) = 4.917 - 41631.1\, e^{-5.243r}(r - 0.971816)(1.03617 + r(r - 1.81663)) + \frac{0.5}{z^{12}} - \frac{7.15109}{z}$$

The Neutral NO potential is modeled in a similar 2-D fashion. Here the r-dependence is based on a Rydberg Function (somewhat more flexible than a Morse potential) and fitting constants determined by Huxley and Murrell in Ref. S2.

$$V_{NO}(r) = 6.614 - 15908.4\, e^{-5.398r}(r - 0.895928)(0.749842 + r(r - 1.09722))$$

The z-dependence is modeled with a repulsive wall and a shallow minimum

$$V_{NO}(z) = \frac{1.5}{r^{12}} + e^{-1.5r}(3.19824 - 2.59317r)$$

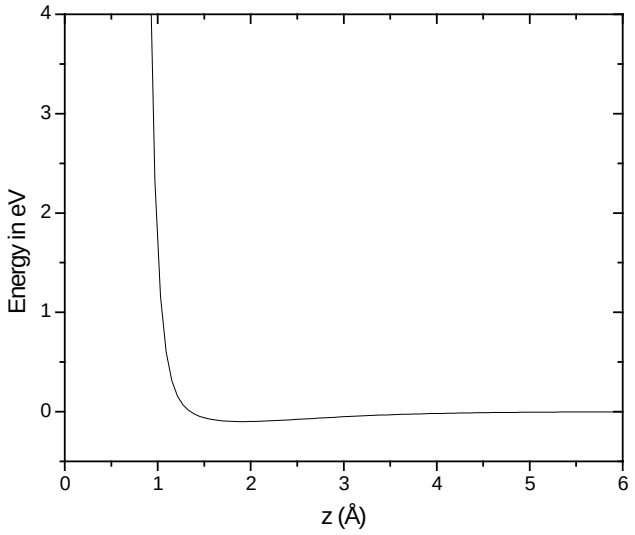

Likewise, the Neutral 2-D potential was constructed as for the anion.

$$V_{NO}(r,z) = V_{NO}(r) + V_{NO}(z) = 6.614 - 15908.4\, e^{-5.398r}(r - 0.895928)(0.749842 + r(r - 1.09722)) + \frac{1.5}{z^{12}} + e^{-1.5z}(3.19824 - 2.59317\, z)$$

The two (anion vs. neutral) potentials are offset with respect to one another by the electron transfer energetics, Φ-EA. The anion potential has been adjusted upward by 0.24 eV to accurately reproduce the O-atom electron affinity at large values of r. This is due to the *ab initio* calculations' error in the dissociation energy of the anion. There is some ambiguity in this adjustment as the accuracy of the NO electron affinity is thereby impacted. However, making adjustments to this model to ensure accuracy of the EA of NO at the expense of the EA of O, does not significantly change the outcome.

Next, we show a cut through the 2D potentials at large values of z. This is shown as Figure 3a in the main text. We envision that at the outer turning point of vibration (1.6Å) a vertical transition releases (wastes) a small (~0.4 eV) amount of energy, promoting an electron from 0.4 eV below the Fermi Level to NO's LUMO. At the inner turning point of vibration (1.089 Å) the

energy release, ΔE_2, depends on distance from the surface and drops below the surface work function at about z=5Å. This result can be seen in the Figure below.

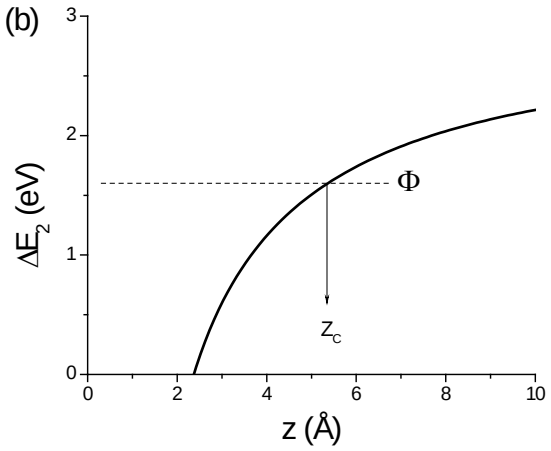

This is the basis for invoking a critical distance z_c~5Å. One might also imagine that the electron transfer at the outer turning point takes place adiabatically. This is the case described in the paper. Thus no energy is "wasted" in the initial electron transfer. In this case the energy available to eject the electron is somewhat larger and the approach to the surface can be somewhat closer before the image charge interaction prevents charge ejection. This is shown by the dotted line in the figure below. Thus there is an '*outer turning point adiabatic*' (dotted lines in figure below) critical distance and an '*outer turning point nonadiabatic*' (solid lines in figure below) critical distance. These differ however by little.

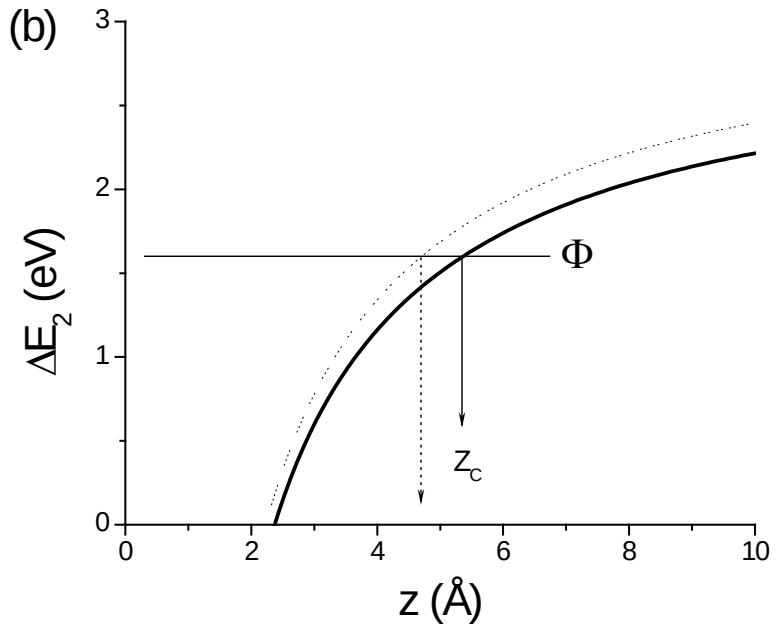

According to Shenvi et al. (S3) the tunneling coupling matrix element can be modeled by the function.

$$V(\varepsilon) \sim e^{-z\sqrt{\frac{2m_e(\Phi-\varepsilon)}{\hbar^2}}}$$

This shows that the tunneling coupling near the critical distance is significant. See Figure below (dotted line).

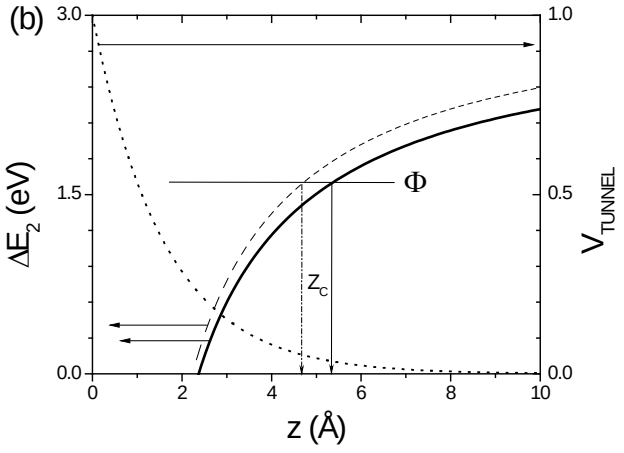

Here a work function of 1.6 eV was used and the energy of the Fermi level (ε=0) was used.

REFERENCES

S1. M. C. McCarthy, J. W. R. Allington, K. S. Griffith, *Chem. Phys. Lett.* **289**, 156 (1998).
S2. P. Huxley, J. N. Murrell, *J. Chem. Soc. - Faraday Transactions II* **79**, 323 (1983).
S3. N. Shenvi, S. Roy, P. Parandekar, J. Tully, *J. Chem. Phys.* **125**, 154703 (2006).